J Mater Sci: Mater Med (2015) 26:177
DOI 10.1007/s10856-015-5516-1

Effect of a new bioactive fibrous glassy scaffold on bone repair

P. R. Gabbai-Armelin[1,5] · M. T. Souza[2] · H. W. Kido[1,5] · C. R. Tim[1,5] · P. S. Bossini[3] · A. M. P. Magri[3] · K. R. Fernandes[3] · F. A. C. Pastor[4] · E. D. Zanotto[2] · N. A. Parizotto[5] · O. Peitl[2] · A. C. M. Renno[3]

Received: 23 May 2014 / Accepted: 11 March 2015 / Published online: 17 April 2015

Abstract Researchers have investigated several therapeutic approaches to treat non-union fractures. Among these, bioactive glasses and glass ceramics have been widely used as grafts. This class of biomaterial has the ability to integrate with living bone. Nevertheless, bioglass and bioactive materials have been used mainly as powder and blocks, compromising the filling of irregular bone defects. Considering this matter, our research group has developed a new bioactive glass composition that can originate malleable fibers, which can offer a more suitable material to be used as bone graft substitutes. Thus, the aim of this study was to assess the morphological structure (via scanning electron microscope) of these fibers upon incubation in phosphate buffered saline (PBS) after 1, 7 and 14 days and, also, evaluate the in vivo tissue response to the new biomaterial using implantation in rat tibial defects. The histopathological, immunohistochemistry and biomechanical analyzes after 15, 30 and 60 days of implantation were performed to investigate the effects of the material on bone repair. The PBS incubation indicated that the fibers of the glassy scaffold degraded over time. The histological analysis revealed a progressive degradation of the material with increasing implantation time and also its substitution by granulation tissue and woven bone. Histomorphometry showed a higher amount of newly formed bone area in the control group (CG) compared to the biomaterial group (BG) 15 days post-surgery. After 30 and 60 days, CG and BG showed a similar amount of newly formed bone. The novel biomaterial enhanced the expression of RUNX-2 and RANK-L, and also improved the mechanical properties of the tibial callus at day 15 after surgery. These results indicated a promising use of the new biomaterial for bone engineering. However, further long-term studies should be carried out to provide additional information concerning the material degradation in the later stages and the bone regeneration induced by the fibrous material.

✉ P. R. Gabbai-Armelin
paulogabbai@gmail.com

[1] Federal University of São Carlos (UFSCar), Rodovia Washington Luís (SP-310), km 235, São Carlos, SP, Brazil

[2] Vitreous Materials Laboratory (LaMaV), Department of Materials Engineering, Federal University of São Carlos (UFSCar), Rodovia Washington Luís (SP-310), km 235, São Carlos, SP, Brazil

[3] Department of Biosciences, Federal University of São Paulo (UNIFESP), Avenida Ana Costa 95, Santos, SP, Brazil

[4] Department of Physiological Sciences, Federal University of São Carlos (UFSCar), Rodovia Washington Luís (SP-310), km 235, São Carlos, SP, Brazil

[5] Department of Physiotherapy, Federal University of São Carlos (UFSCar), Rodovia Washington Luís (SP-310), km 235, São Carlos, SP, Brazil

1 Introduction

Bone is one of the most replaced tissues of the body, with more than 500,000 bone graft procedures performed per year only in the USA [1, 2]. In this context, researchers have investigated different solutions to treat non-union fractures and a series of bone replacement graft materials has been extensively used with varying degrees of success, such as autografts, allografts and synthetic bone substitutes [3, 4].

The use of autologous bone grafts as bone substitutes is considered the gold standard, but their use involves several problems, such as donor site morbidity, the need of additional surgeries, and the relative small amounts of available bone [5]. An alternative is the use of allogenic bone grafts, but their utilization is limited by the risks of rejection and

transmission of diseases [6]. Widespread interest has, therefore, focused on the development of synthetic bone substitutes, including mainly hydroxyapatite (HA), calcium phosphate (CaP) ceramics [7] and polymer-based materials [8].

Also, bioactive glasses (BGs) have been widely used as bone substitutes and grafts [9]. It is a class of biomaterials that undergoes a series of surface reaction when in contact with fluids, forming a biologically active bone-like apatite layer on their surfaces [10]. BGs are absorbable and their dissolution products (soluble silicon and calcium) have been found to up-regulate seven families of genes in osteoblasts [11]. The original bioactive glass developed by Hench and named Bioglass® 45S5 is a melt-derived glass with four components (46.1 % SiO_2, 24.4 % Na_2O, 26.9 % CaO and 2.6 % P_2O_5, in mol). Bioglass® 45S5 has been known for many years as the most bioactive composition among numerous bone-bonding glasses. It has been used in many clinical procedures, including the repair of periodontal bone defects, maxillofacial defects reconstruction, spinal surgery and bone replacement [11, 12].

Bioglass and bioactive materials have been used mainly in powders and blocks [13, 14]. Although, in most cases these materials permit and support cell migration and angiogenesis, they do not have the ability of acting as fillers for bone defects with irregular shapes [15]. In this context, moldability, such as the one found in fibrous materials, is a desirable characteristic required for grafts, allowing to fit irregular bone defects [16]. Functional fibrous substrates will support cell attachment, proliferation and differentiation at the region of the defect, which permit cells to secrete extracellular matrix (ECM) for mineralization in order to form bone [17]. Poologasundarampillai produced a fibrous glassy scaffold (SiO_2–CaO), via sol–gel and electrospinning, and observed that a hydroxycarbonate apatite (HCA) layer was formed on the fibers within 12 h upon incubation in simulated body fluid. Additionally, the fibrous glassy material showed no cytotoxic effect in culture with MC3T3 and the cells were observed to attach to and spread in the material [18]. Studies conducted by Lin showed that copper-containing borate glass fibers implanted subcutaneously in rats promoted extensive angiogenesis compared to 45S5 and to the sham group. Cytotoxicity was also assessed via histological evaluation, but no histopathological changes were observed. These results indicated that the fibrous glassy material is safe and effective for tissue regeneration applications [19]. Thus, the obtainment of malleable fibers from bioactive glasses seems to be a promising therapeutic approach to be used for bone repair.

Toward this goal, fibrous glassy scaffolds, belonging to the SiO_2–Na_2O–K_2O–MgO–CaO–P_2O_5 system, have been recently developed (Patent Application BR 10 2013 020961 9; Fundação Universidade Federal de São Carlos, 2013) [20]. The new fibrous material combines malleability with the high bioactivity of BGs, expanding the potential applications of the biomaterial.

Since there is a growing interest in the development of materials with improved osteogenic properties, it was hypothesized that this fibrous glassy scaffold would have improved in vivo bioactive properties and more adequate morphology to facilitate cell migration and vascularization, providing a bone graft with additional advantages for clinical use. Consequently, the present study aimed to assess the morphological structure of these fibrous glassy scaffolds and evaluate the temporal in vivo response of this novel biomaterial in a tibial bone defect model in rats. To this end, scaffolds were analyzed via SEM and, also, implanted into created non-critical bone defects in rats. Histopathological, immunohistochemistry and biomechanical analyzes were evaluated after 15, 30 and 60 days of implantation.

2 Methodology

2.1 Fibrous glassy scaffolds

The fibrous scaffolds were obtained from a brand new highly bioactive glass developed by researchers of the Vitreous Materials Laboratory (LaMaV), Department of Materials Engineering, Federal University of São Carlos, São Carlos, São Paulo, Brazil. The bioactive glass belongs to the SiO_2–Na_2O–K_2O–MgO–CaO–P_2O_5 system and was prepared by melting the chemical reagents at 1200 °C in a platinum crucible, crushed and remelted at 1200 °C to provide homogenization. After the glass was produced, bioactive fibers were manufactured in a homemade fiber tower. After this procedure, highly porous circular scaffolds (3 mm × 1 mm) were obtained using chopped fibers. These fibers were weighed and put in a cylindrical polytetrafluoroethylene mold to obtain disc shaped samples. The structure of the scaffolds was evaluated using SEM (Phenom™, FEI, Company).

2.2 Morphology after incubation in phosphate buffered saline (PBS)

The morphology of the fibrous glassy scaffold—after 1, 7 and 14 days of immersion in PBS—was determined using SEM (LEO 440, LEO Electron Microscopy Ltda). The degradation behavior of the scaffolds was visualized at various magnifications.

2.3 Experimental design

In this study, 60 male Wistar rats (aged 12 weeks and weighing 250–300 g) were used. They were maintained

under controlled temperature (24 ± 2 °C), light–dark periods of 12 h, with unrestricted access to water and commercial diet. Each animal handling and surgical procedures were strictly conducted according the Guiding Principles for the Use of Laboratory Animals. This study was approved by the Animal Care Committee guidelines of the Federal University of São Carlos (Protocol 043/2012).

Animals were divided into two groups: bone defect control group (CG), in which the bone defects received no filler, and the biomaterial group (BG), in which the bone defects were filled with fibrous scaffolds. Each group was divided into three different sub-groups (N = 10) sacrificed in different periods (15, 30 and 60 days after surgery). As described below, a non-critical size bone defect was performed on both tibias.

2.4 Surgical procedures

All surgical procedures were performed under sterile conditions and general anesthesia was induced by intra-peritoneal injection of Ketamine/Xylazine (80/10 mg/kg). Buprenorfine (Temgesic; Reckitt Benckiser Health Care Limited, Schering-Plough, Hoddesdon, UK) was administered intraperitoneally (0.02 mg/kg) directly after the operation and subcutaneously for 2 days after surgery, to minimize post-operative discomfort.

To insert implants into the tibial defects, the animals were immobilized and both hind limbs were shaved, washed and disinfected with povidone-iodine. The medial compartment of the tibia was exposed through a longitudinal incision on the shaved skin. After exposure, a 1.0 mm pilot hole was drilled. The hole was gradually widened with drills of increasing size until a final defect size of 3 mm in width and 3 mm in depth was reached. Low rotational drill speeds (max. 450 rpm) and constant physiologic saline irrigation were used. Surgery was performed bilaterally and one defect was created in each tibia. Immediately, a sterilized 3.0 mm diameter fibrous scaffold was implanted in the bone cavities, with the exception of control animals. After implantation, the cutaneous flap was replaced and sutured with absorbable Vicryl® 5-0 (Johnson&Johnson, St.Stevens-Woluwe, Belgium), and the skin was disinfected with povidone iodin. The health status of all animals was monitored daily.

On days 15, 30 and 60 post-surgery, rats were euthanized individually by carbon dioxide asphyxia. The tibias were defleshed and removed for analysis.

2.5 Histopathological analysis

In the histopathological and immunohistochemistry analysis, the right tibiae were removed and fixed in 10 % buffer formalin (Merck, Darmstadt, Germany) for 24 h. They were decalcified in 4 % EDTA (Merck) and embedded in paraffin blocks. Five-micrometer slices were obtained perpendicular to the medial–lateral drilling axis of the implant using a microtome (Leica Microsystems SP 1600, Nussloch, Germany). At least, three sections of each specimen were stained with hematoxylin and eosin (H.E stain, Merck). Histopathological evaluation was performed under an optical microscope (Olympus, Optical Co. Ltd, Tokyo, Japan). The area of the bone defect was qualitatively evaluated considering the inflammatory process, granulation tissue and newly formed bone. At least three sections of each specimen were examined using light microscopy (Leica Microsystems AG, Wetzlar, Germany).

Additionally, morphometry analysis was performed and, in order to do that, histological sections were quantitatively evaluated via computer-based image analysis techniques (Axioplan 2, Carl Zeiss, Jena, Germany). Digitalized images of the defect (×20) were obtained and the amount of newly formed bone was determined within three regions of interest: ROI1 (upper left border), ROI2 (lower left border), and ROI3 (central region of the right border) [21, 22]. The total amount of newly formed bone was represented as ROI1 + ROI2 + ROI3 (in square micrometer). Two experienced observers (PRGA and ACMR) performed the analysis in a blinded manner.

2.6 Immunohistochemistry

For the immunohistochemistry analysis, xylene was used to remove the paraffin from the serial sections of 5 μm. After this procedure, the sections were rehydrated in graded ethanol and pretreated in a microwave (Electrolux, São Paulo, Brazil) with 0.01 M citric acid buffer (pH 6) for three cycles of 5 min each at 850 W for antigen retrieval. The resulting material was pre-incubated with 0.3 % hydrogen peroxide in PBS solution for 5 min in order to inactivate the endogenous peroxidase. Then, the samples were blocked with 5 % normal goat serum in PBS for 10 min. The specimens were incubated with anti-RUNX-2 polyclonal primary antibody (code: sc-8566, Santa Cruz Biotechnology, USA) at a concentration of 1:200, anti-RANK-L polyclonal primary antibody (code: sc-7627, Santa Cruz Biotechnology, USA) at a concentration of 1:200, and anti-COL-1 polyclonal primary antibody (code: sc-8784, Santa Cruz Biotechnology, USA) also at a concentration of 1:200. Incubation was carried out overnight at 4 °C into a refrigerator. This step was followed by two washes in PBS for 10 min. The sections were then incubated with biotin conjugated secondary antibody anti-rabbit IgG (Vector Laboratories, Burlingame, CA, USA) at a concentration of 1:200 in PBS for 1 h. The sections were washed twice with PBS followed by the application of preformed avidin biotin complex conjugated to peroxidase

(Vector Laboratories) for 45 min. The bound complexes were visualized by the application of a 0.05 % solution of 3-3′-diaminobenzidine solution and counterstained with Harris hematoxylin (Sigma-Aldrich). For control studies of the antibodies, the serial sections were treated with rabbit IgG (Vector Laboratories) at a concentration of 1:200 in place of the primary antibody. Additionally, internal positive controls were performed with each staining bath.

RUNX-2, RANK-L and COL-1 immunoexpressions were evaluated qualitatively and quantitatively. The qualitative analysis was performed in order to assess the presence (or absence) and region of occurrence of the immunomarkers. Regarding the quantitative investigation, this analysis was performed to evaluate the immunolabeling intensity of each immunomarker, in four predetermined fields inside the defect, according to a previously described scoring scale from 1 to 4 (1 = absent, 2 = weak, 3 = moderate and 4 = intense) [23, 24]. The analysis was performed by two observers (PRGA and KRF) in a blinded way using a light microscopy (Leica Microsystems AG, Wetzlar, Germany).

2.7 Mechanical test

The biomechanical properties of the left tibia were determined by a three-point bending test performed in an Instron® Universal Testing Machine (USA, 4444 model, 1 KN load cell). The tibiae were placed on a 3.8-cm metal device, which provided a 1.8-cm-distant double support on the bone diaphysis. The load cell was perpendicularly positioned at the exact site of the bone defect. A 5 N pre-load was applied in order to avoid specimen sliding. Finally, the bending force was applied at a constant deformation rate of 0.5 cm/min until fracture occurred. The maximum load (N) at the failure was obtained from the load-deformation curve.

2.8 Statistical analysis

The normality of all variable distribution was verified using Shapiro–Wilk's W test. For the variable that exhibited normal distribution, comparisons among the groups were made using one-way analysis of variance (ANOVA), complemented by Tukey post-test analysis. STATISTICA version 7.0 (data analysis software system - StatSoft Inc.) was used to carry out the statistics analysis. Values of $P < 0.05$ were considered statistically significant.

3 Results

3.1 Morphology of the fibrous glassy scaffold

The structure of the fibrous scaffold was analyzed through SEM. Figure 1 shows that the fibers of the scaffold were randomly positioned. The glass-shaped fibers constitute a very porous biomaterial with interconnected pores, presenting sufficient mechanical strength for handling. The mean fiber diameter was 42.2 with a standard deviation of ±5.1 μm.

3.2 Morphology after incubation

SEM micrographs indicated signs of initial degradation of the fibers upon immersion in PBS after 1, 7 and 14 days (Fig. 2). Ruptures, related to the degradation, were observed in the structures of the fibers over time.

3.3 General findings post-implantation

A number of 30 animals were used for the BG. From this number, three animals were lost because of respiratory depression induced by anesthesia. For the remaining animals, neither postoperative complications nor behavioral changes were observed. The rats returned rapidly to their normal diet and showed no loss of weight in the experimentation (data not shown). Moreover, during the experiment, no infection in the surgical site was observed. After the later experimental period, 54 tibial implants were retrieved, of which 48 were included for analyzes (six implants were lost due to tibia or implant fractures during histological procedures). Table 1 presents an overview of the number of implants that were placed, retrieved and used for analysis.

3.4 Histopathological analysis of tibial implants

3.4.1 15 Days

Representative histological sections of all experimental groups after implantation are depicted in Fig. 3 (magnification of

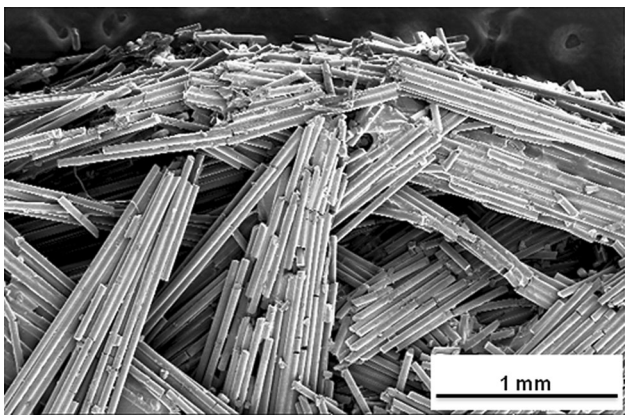

Fig. 1 SEM image of the fibrous glassy scaffold. Magnification of ×35

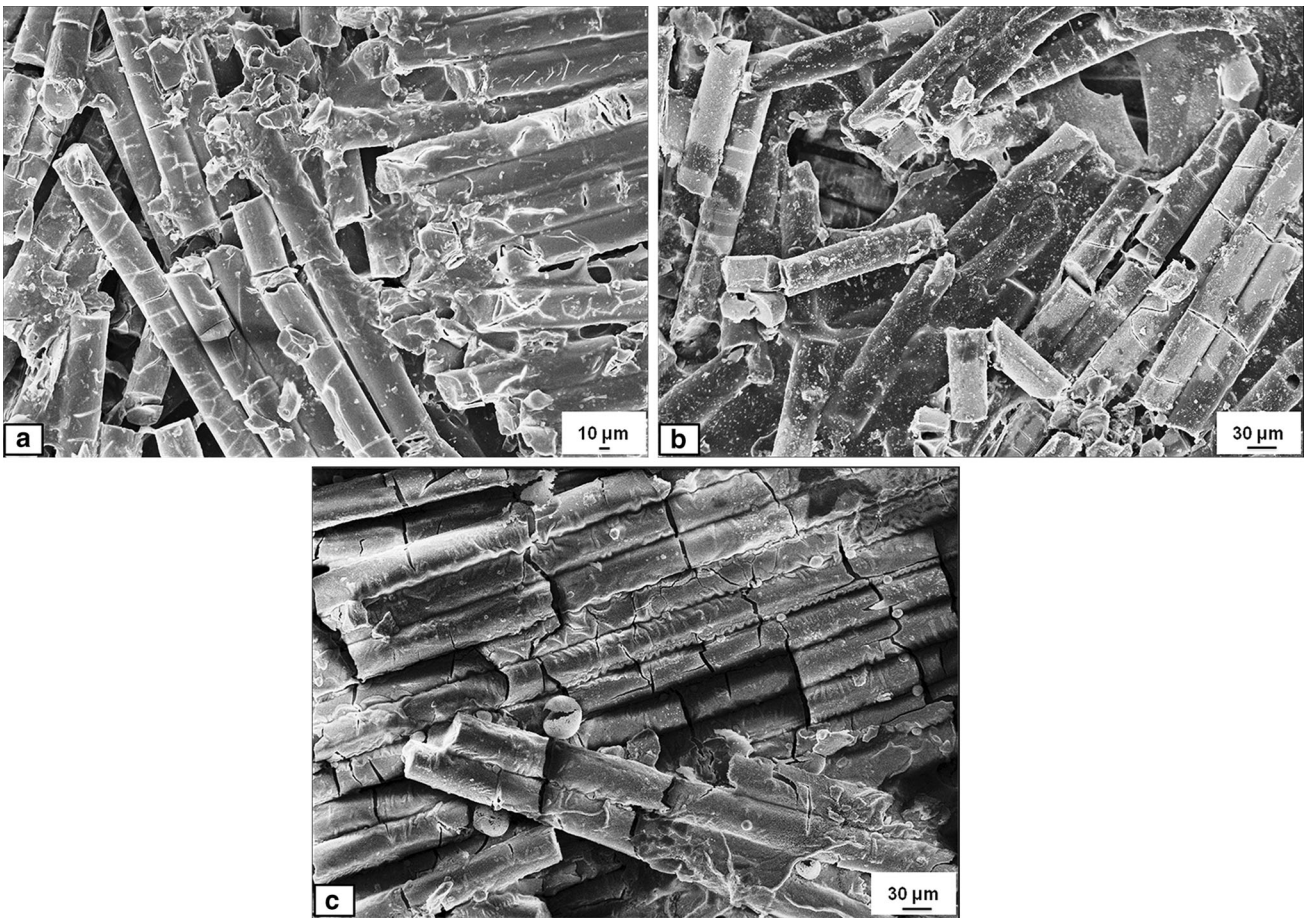

Fig. 2 SEM micrographs of the fibrous glassy scaffold for up to 14 days post-incubation in PBS. **a** 1 day; **b** 7 days and **c** 14 days. Magnification of ×500

Table 1 Implants placed, retrieved and used for histological and immunohistochemistry analyzes

	Implants placed	Implants retrieved	Implants used for analyzes
15 Days	20	18[a]	16[b]
30 Days	20	20	18[b]
60 Days	20	16[a]	14[b]

[a] Deviation versus implants placed due to animal dead

[b] Deviation versus implants retrieved due to tibial or implant fractures

×10). Fifteen days post-surgery, histology assessment revealed that the bone defect was almost completely filled with the biomaterial, which presented signs of initial degradation (Fig. 3a).

Figure 4 shows the histological findings at a higher magnification. It was noticed, for CG and BG, granulation tissue with discrete inflammatory process at the site of the defect (Fig. 4a, b). For both groups, it was also observed the presence of an early woven bone organization in the periphery of the defect. Histological analysis revealed signs of material degradation, although an intense presence of the biomaterial still could be observed (Fig. 4a). The degraded area of the implant allowed the ingrowth of soft tissue around the fibers of the scaffolds.

3.4.2 30 Days

The material degradation has continued after 30 days of implantation and newly formed bone replaced the area previously occupied by the material (Fig. 3b). At a higher magnification, no inflammatory process was observed either for CG or BG (Fig. 4c, d). For CG, a minor amount of granulation tissue and newly formed bone were observed at the region of the defect (Fig. 4c). Compared to the

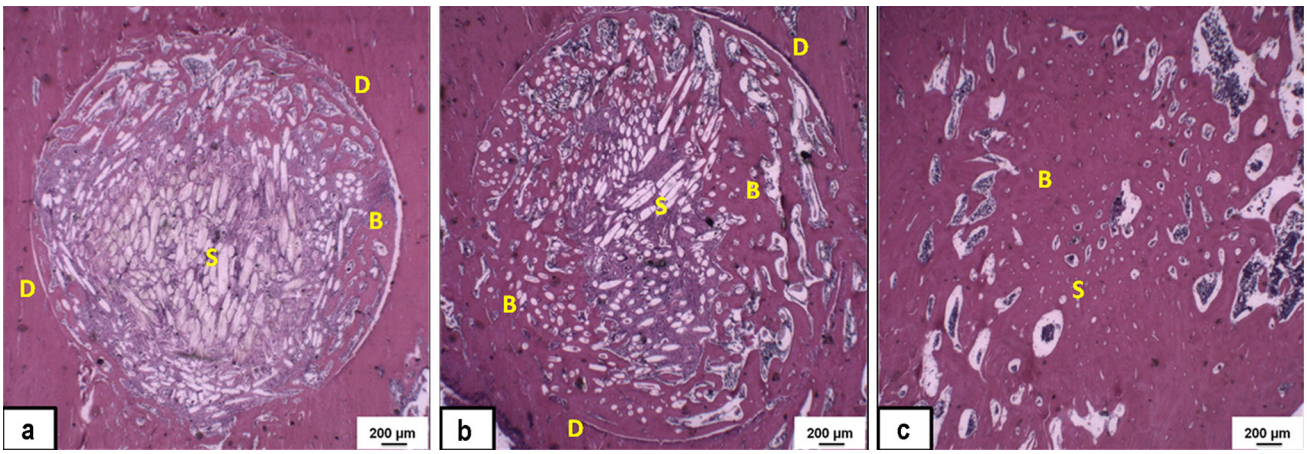

Fig. 3 Tibial defects. Representative histological sections of BG in the 3 experimental periods: 15 days (**a**), 30 days (**b**), and 60 days (**c**). Fibers of the porous scaffold (*S*), bone formation (*B*), and defect line (*D*) are indicated in the sections. *Bar* represents 200 μm. Hematoxylin–eosin staining. Magnification of ×12.5

experimental period of 15 days, BG showed lower amounts of granulation tissue (mostly located in the central region of the scaffold). It was also noticed organized newly formed bone substituting the degraded material (Fig. 4d). The borders of the defects were still delimited for both groups.

3.4.3 60 Days

Figure 3c shows that 60 days after the implantation, the material was almost completely degraded and a mature formed bone occupied the defect (Fig. 3c). At a higher magnification, no inflammatory process or granulation tissue were noticed for CG and BG (Fig. 4e, f). In this period, both groups presented bone remodeling in the defect site. In BG, the borders of the defect were not noticed anymore in most cases, and some fibers still could be observed.

3.5 Histomorphometrical analysis

Histomorphometrical analysis revealed that, after 15 days of implantation, BG showed a significant decrease in the amount of newly formed bone compared to CG (21.3 ± 2.4 and 46.8 ± 7.1 % respectively; $P < 0.05$). After 30 and 60 days, however, CG and BG showed similar amount of newly formed bone at the site of the injury ($P > 0.05$; Fig. 5).

3.6 Immunohistochemistry

3.6.1 Qualitative analysis

Regarding CG, after 15 and 30 days of implantation, the immunostaining for RUNX-2 was noticed mainly in the medullar tissue and in osteoblasts in the periphery of bone defect (Fig. 6a, c, e). Sixty days post-surgery, the labeling for RUNX-2 was observed mainly in the remaining medullar tissue and in the newly formed bone (Fig. 6e). Concerning BG, after 15 and 30 days post-surgery, the labeling for RUNX-2 was identified throughout the defect, being more evident in the central area among the fibers of the biomaterial (Fig. 6b, d, e). Still in the treated group, on day 60, the immunoexpression of RUNX-2 was also in the medullar tissue and in some regions of the neoformed bone (Fig. 6f).

RANK-L expression in CG was detected predominantly in the medullar tissue and in the border of the defect in all experimental groups (Fig. 7a, c, e). In BG, after 15 and 30 days post-surgery, the labeling for RANK-L was observed in the entire defect, mainly in the granulation tissue around the fibers of the biomaterial (Fig. 7b, d, e). At the last set point evaluated in BG, the immunoexpression of RANK-L was observed around the borders of the newly formed bone (Fig. 7f).

Regarding the COL-1 expression, CG of all periods presented immunoreactivity throughout the neoformed bone (Fig. 8a, c, e). In the case of BG, at 15 and 30 days post-implantation, the expression was detected mostly in the neoformed bone on the border of defect (Fig. 8b, d). In the last experimental period, the immunolabeling of COL-1 could be noticed in the entire defect, since it was completely filled with newly formed bone (Fig. 8f).

3.6.2 Quantitative analysis

The immunolabeling for RUNX-2 at days 15 and 30 after surgery was significantly higher in BG compared to CG (Fig. 9a). In the case of RANK-L, this immunomarker had a higher expression in BG compared to CG, 30 and 60 days after implantation (Fig. 9b). Similar findings for COL-1 expression were noticed in CG and BG at different experimental periods analyzed (Fig. 9c).

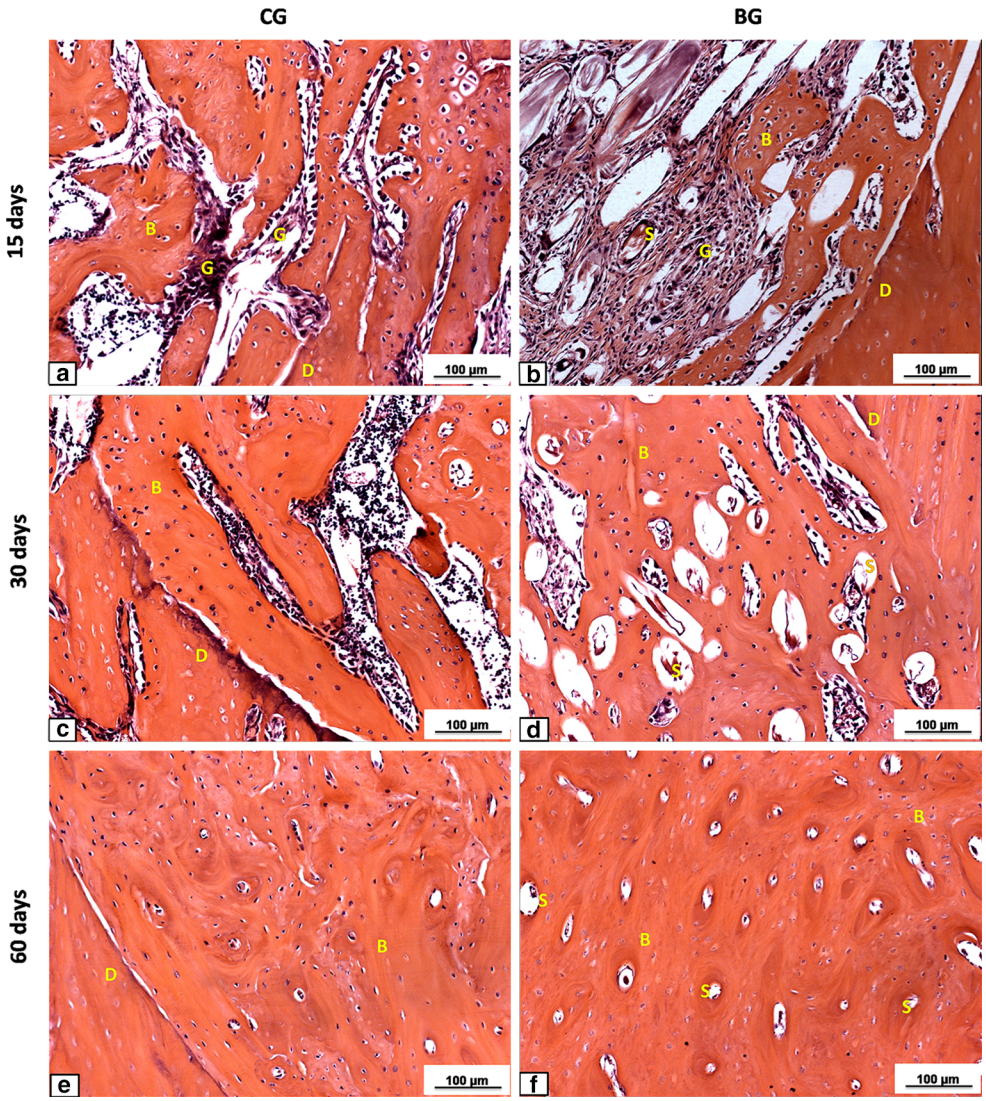

Fig. 4 Representative histological sections of CG and BG in the 3 experimental periods; CG: 15 days (**a**), 30 days (**c**), and 60 days (**e**); BG: 15 days (**b**), 30 days (**d**), and 60 days (**f**). Granulation tissue (*G*), fibers of the porous scaffold (*S*), bone formation (*B*), and defect line (*D*) are indicated in the sections. *Bar* represents 100 µm. Hematoxylin–eosin staining. Magnification of ×200

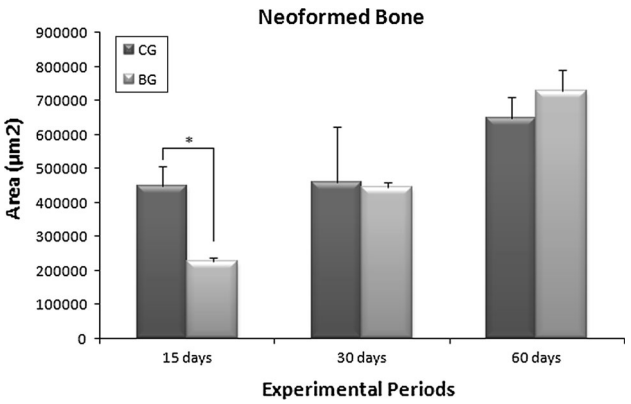

Fig. 5 Means and standard error of the mean of the morphometry assessment. Significant differences of $P < 0.05$ are represented by an *asterisk*

3.7 Mechanical test

The biomechanical analysis showed statistically difference in the maximal load comparing BG to CG at day 15 after surgery, with a significantly increase in the treated group (Table 2). No difference between CG and BG was observed for the other analyzed variables.

4 Discussion

The aim of this study was to assess the morphology of the fibrous glassy scaffold and investigate the in vivo tissue response of this biomaterial. For this purpose, the scaffolds were evaluated via SEM and, also, implanted into tibial

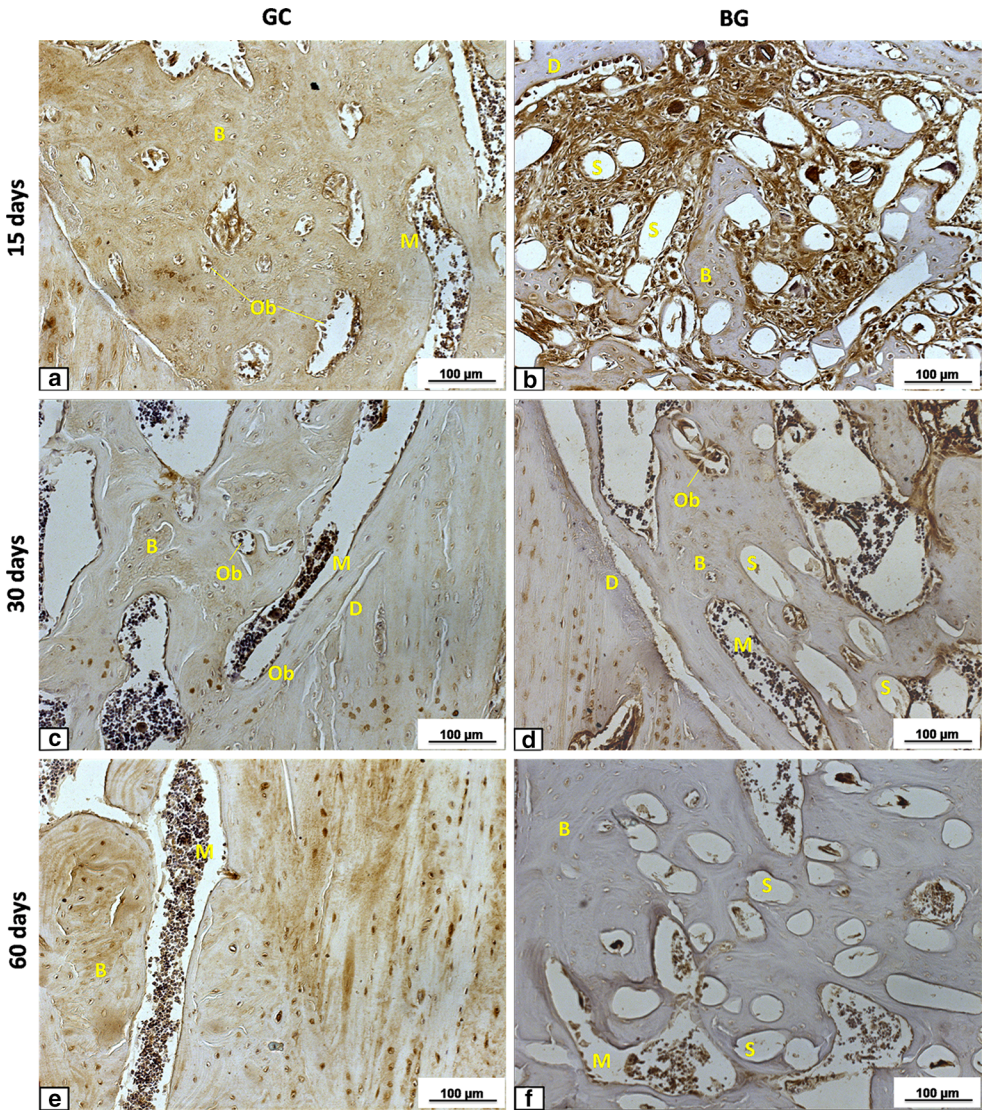

Fig. 6 Immunohistochemistry of RUNX-2. CG: 15 days (**a**), 30 days (**c**), and 60 days (**e**); BG: 15 days (**b**), 30 days (**d**), and 60 days (**f**). Fibers of the porous scaffold (*S*), bone formation (*B*), medullar tissue (*M*), osteoblasts (*Ob*), and defect line (*D*) are indicated in the sections. *Bar* represents 100 µm. Magnification of ×200

bone defects and analyzed after 15, 30 and 60 days. The hypothesis was that the fibrous bioactive material would present an appropriate structure and an adequate bioactivity to permit bone cell growth and bone formation. SEM micrographs showed that the fibrous glassy scaffold constitutes a very porous biomaterial with interconnected pores, degrading over time upon immersion in PBS. Histology revealed that the material degraded at the site of the injury with increasing time, allowing bone ingrowth. Histomorphometry analysis demonstrated that the newly formed bone area in CG was higher than BG, 15 days post-surgery. However, no difference was found in the other experimental periods. In addition, the BG showed an upregulation of RUNX-2 and RANK-L expression, and increased maximal load values 15 days post-surgery.

SEM evaluation of the scaffold's morphology after incubation indicated an initial degradation over time accompanied by ruptures in the structures of the fibers. These breaks might be beneficial since it increases degradation of the scaffold, allowing the substitution of the material by bone tissue [25, 26].

Furthermore, the histological findings also revealed a degradation of the material with increasing implantation time, and its substitution by granulation tissue and newly formed bone. Such data are in line with previous studies conducted by our group, which investigated the effects of a glass–ceramic biomaterial, with similar chemical compositions (Biosilicate®, P_2O_5–Na_2O–CaO–SiO_2), on bone formation in rat tibial defects. Likewise these studies showed a degradation of Biosilicate® over time, followed

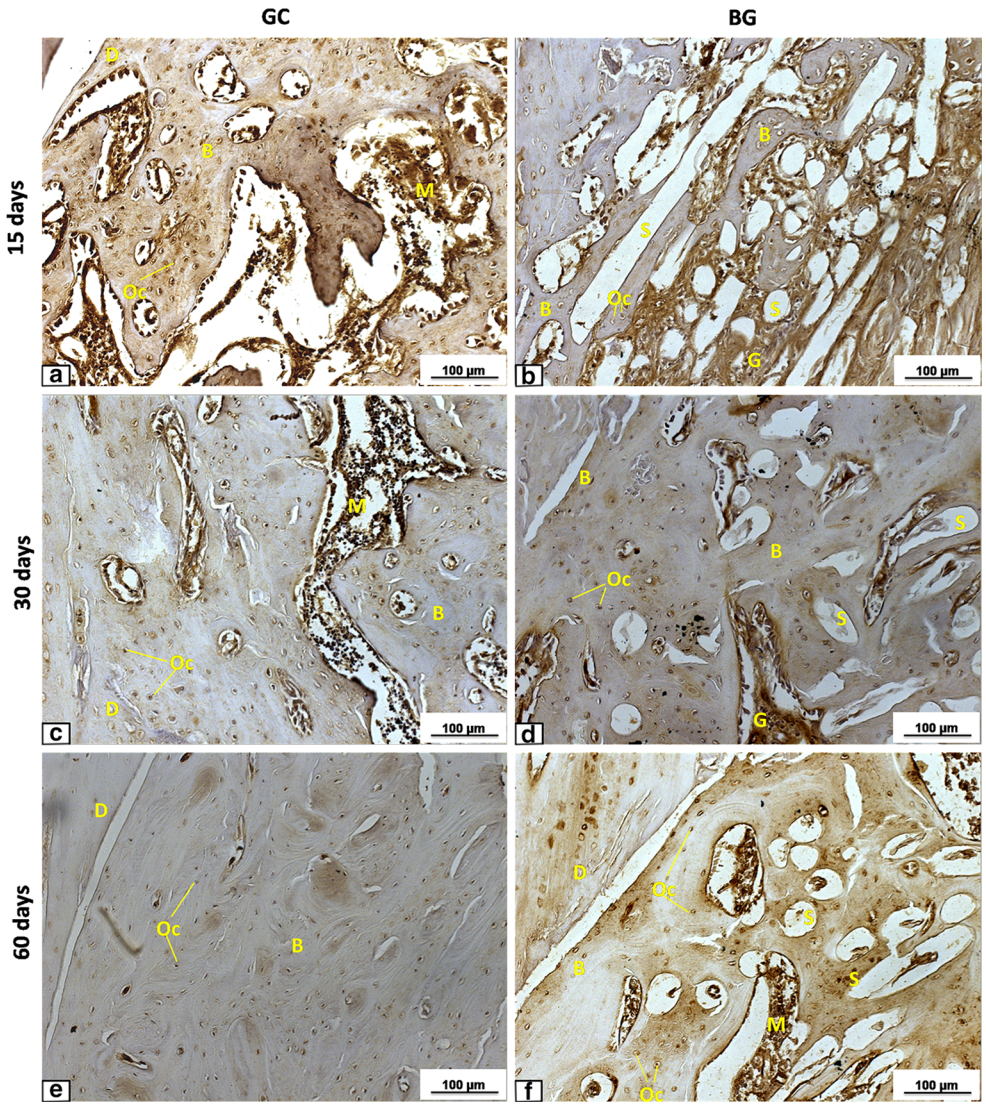

Fig. 7 Immunohistochemistry of RANK-L. CG: 15 days (**a**), 30 days (**c**), and 60 days (**e**); BG: 15 days (**b**), 30 days (**d**), and 60 days (**f**). Granulation tissue (*G*), fibers of the porous scaffold (*S*), bone formation (*B*), medullar tissue (*M*), osteocytes (*Oc*), and defect line (*D*) are indicated in the sections. *Bar* represents 100 µm. Magnification of ×200

by replacement of the material with granulation tissue and woven bone [21, 22].

Bone resorption of material and liberation of space are necessary for tissue ingrowth [27–30]. It seems that the degradation of the highly porous material, found in this study, indeed substantially allowed bone formation. Furthermore, the superior biological properties presented by BG may also be related to the ion dissolution from the fibrous scaffold. Immediately after the contact of the material with fluids, ions are leached and a silica rich layer is formed, acting as a template for calcium phosphate precipitation, and inducing new bone formation [10, 11, 31–33]. These results corroborate those of Renno [34], who tested a porous composite of calcium phosphate cement, poly(D,L-lactic-co-glycolic) acid and Biosilicate® using implantation into femoral condyle defects.

Concerning the immunohistochemistry, it is noteworthy that RUNX-2 expression was higher in BG when compared to CG on days 15 and 30 after implantation. RUNX-2 immunofactor is mainly expressed in osteoblasts and it is required for the differentiation of mesenchymal progenitors toward osteoblast cell lineage. It is well known that RUNX-2 is fundamental for upregulation of other osteoblastic markers, like osteocalcin, osteopontin and alkaline phosphatase [35, 36], which also may have influenced bone formation and deposition. The in vivo findings observed in this study are in agreement with previous studies which have detected higher RUNX-2 immunoexpression in

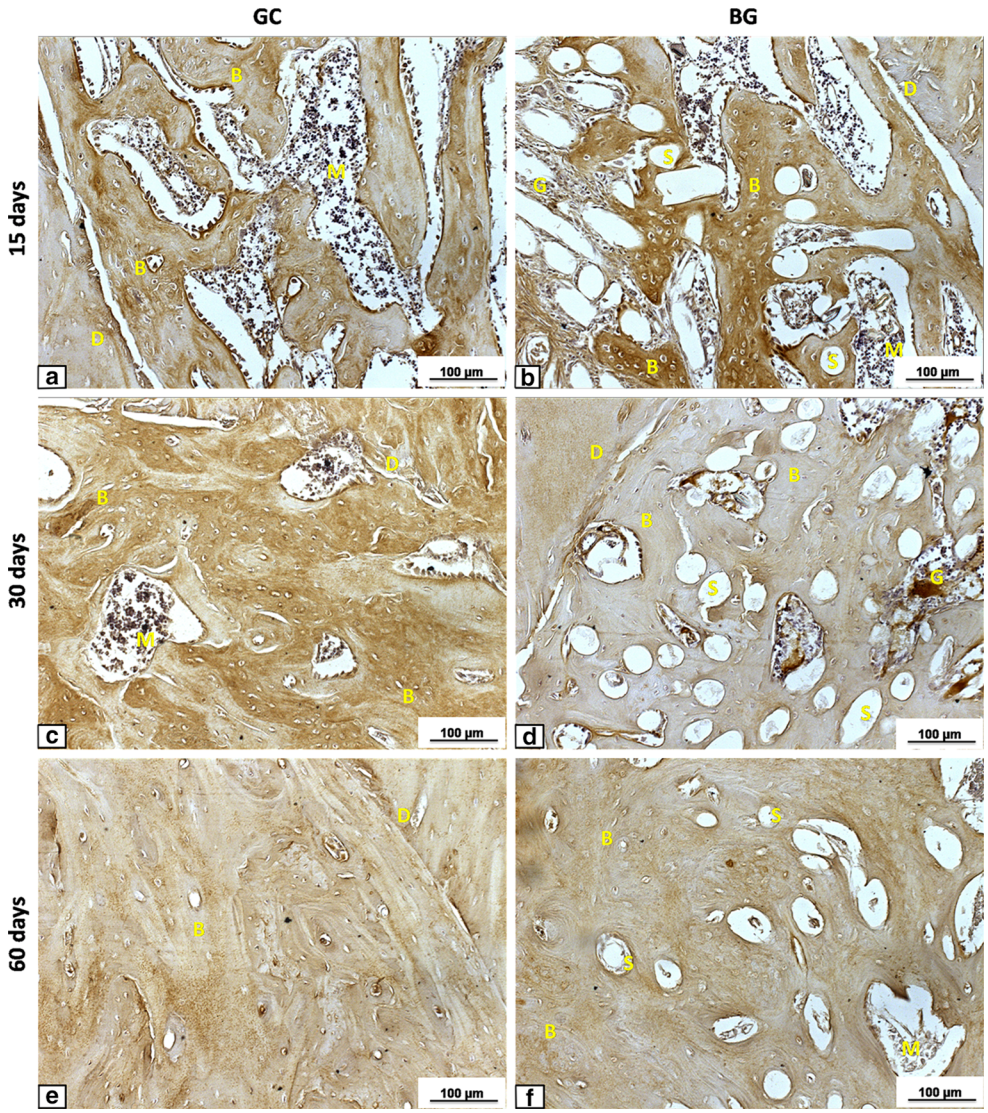

Fig. 8 Immunohistochemistry of COL-1. CG: 15 days (**a**), 30 days (**c**), and 60 days (**e**); BG: 15 days (**b**), 30 days (**d**), and 60 days (**f**). Granulation tissue (*G*), fibers of the porous scaffold (*S*), bone formation (*B*), medullar tissue (*M*), and defect line (*D*) are indicated in the sections. *Bar* represents 100 µm. Magnification of ×200

tibial and calvaria defect models filled with Biosilicate® [22, 24].

Additionally, the resorption and remodeling of bone tissue by osteoclasts is also necessary for a successful bone healing process. In this context, RANK-L is known as a key factor for differentiation and activation of osteoclasts [37–39]. The present study demonstrated a higher immunoexpression of RANK-L in BG, 30 and 60 days post-surgery. Probably, the higher expression of RANK-L indicates an increased presence of osteoclasts in an attempt of degrading the material. Investigations conducted by Pinto [40] verified a more evident immunoexpression of RANK-L around the particles of Biosilicate® glass–ceramic in tibial defects. Similar findings were observed by Kondo [41] who tested b-tricalcium phosphate (b-TCP) using implantation in femoral condyle of rats.

Similarly, COL-1 is the major organic component of bone matrix produced by osteoblasts, and the increase of this protein level is important and critical in mediating the signal cascade for the expression of mature osteoblasts and mineralization of the ECM [42]. Interestingly, in the present study, no statistically significant difference was observed in the COL-1 immunolabeling between the experimental groups. These results do not corroborate those of Valerio [43] who showed that osteoblasts in the presence of ionic products from a bioactive glass (60 % of silica-BG60S) dissolution presented a higher cell proliferation and collagen secretion when compared to control

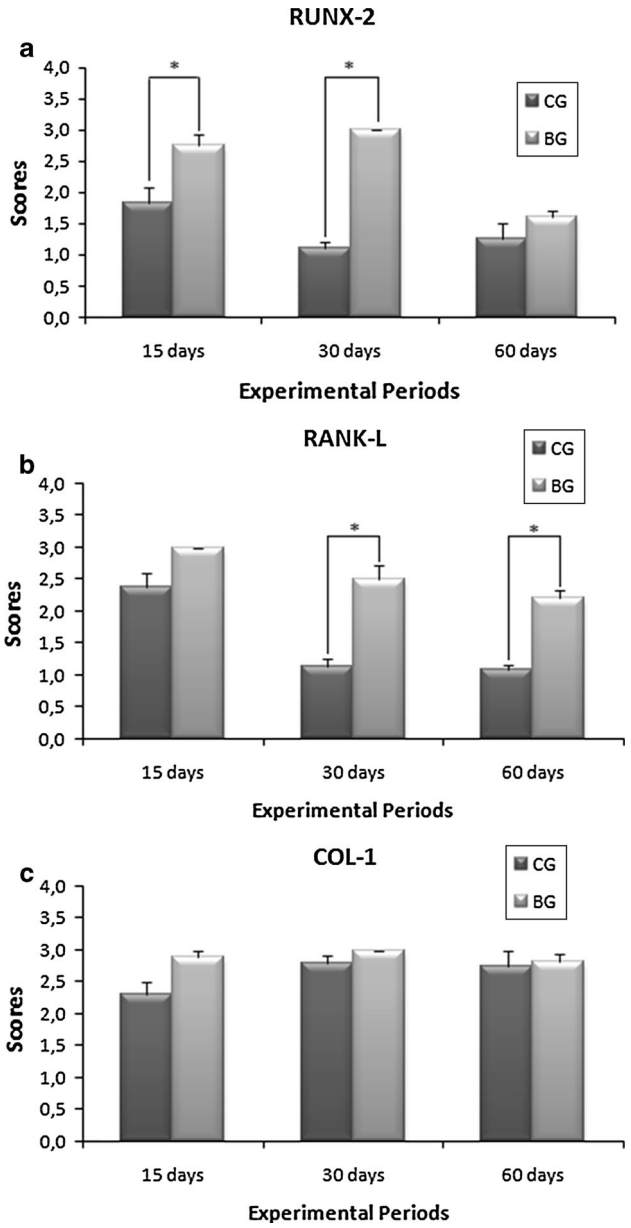

Fig. 9 Means and standard error of the mean for the immunohistochemistry analysis. **a** RUNX-2 **b** RANK-L and, **c** COL-1. Significant differences of $P < 0.05$ are represented by an *asterisk*

group. It is unclear at this stage why the results of the present study occurred, since it was hypothesized that the ionic products of the biomaterial might stimulate collagen organization. In this context, further investigations are necessary to a better understanding of this mechanism.

The mechanical test revealed a higher value of maximal load in the treated group 15 days after the surgery, showing a positive effect in the initial period. Thus, these results show an improvement of the mechanical properties in the tibial callus for the initial group, whose defect was filled with the porous scaffold. This fact may have occurred due to the quality and arrangement of the biomaterial microstructure in the defect, influencing the bone load-bearing capacity. Likewise, Granito [44] evidenced improved mechanical of tibial callus in defects filled with particulate Biosilicate® in comparison with control animals 20 days post-surgery. Regarding other experimental periods, no difference was observed. This fact may be related to the biomaterial degradation, conferring equal amount of newly formed bone with similar tissue organization compared to CG.

The results of the present investigation confirmed our hypothesis that the fibrous glassy scaffold can stimulate bone repair due to its bioactive properties. Nevertheless, once there are differences between the metabolism of healthy bone and the metabolism of compromised conditions (e.g. osteoporosis), the bio-performance of the fibrous porous material might be different and need to be further investigated. Additionally, it would be interesting to evaluate the response of this porous biomaterial in critical-size bone defects (CSD), since in this model the spontaneous bone consolidation does not occur [45]. Thereby, future research is necessary to evaluate this information, as this work was limited to the evaluation of the biomaterial performance under optimal conditions in non-CSDs.

In summary, the results indicated that the fibrous glassy scaffold has potential to be used for bone healing. The novel biomaterial enhanced the expression of osteogenic factors and also improved mechanical properties of the tibial callus at day 15 after surgery. Further long-term

Table 2 Means and standard error of the mean for the biomechanical evaluation of the tibias

	15 Days		30 Days		60 Days	
	CG	BG	CG	BG	CG	BG
Maximal load (kN)	0.048 ± 0.003	0.069 ± 0.005*	0.066 ± 0.004	0.074 ± 0.003	0.073 ± 0.005	0.075 ± 0.007
Resilience (J)	0.034 ± 0.003	0.028 ± 0.002	0.028 ± 0.005	0.029 ± 0.003	0.023 ± 0.003	0.020 ± 0.006
Tenacity (J)	0.043 ± 0.003	0.043 ± 0.006	0.048 ± 0.007	0.038 ± 0.003	0.021 ± 0.006	0.021 ± 0.006

GC control group, *BG* biomaterial group

* $P < 0.05$ compared to CG after 15 days

studies should be carried out to provide additional information concerning the late stages of material degradation and the bone regeneration induced by the fibrous material. Moreover, further research is required to evaluate the biological performance of this new biomaterial in compromised situations to support the use of this promising fibrous material for bone engineering applications.

Acknowledgments The authors are indebted to CAPES, CNPq and FAPESP, São Paulo Research Funding Agency, Grant Number 2013/07793-6 (CeRTEV - Center for Technology, Research and Education in Glass) for funding this research work and PhD students Grant 2011/22937-9.

References

1. Virk MS, Alaee F, Tang H, Ominsky MS, Ke HZ, Lieberman JR. Systemic administration of sclerostin antibody enhances bone repair in a critical-sized femoral defect in a rat model. J Bone Joint Surg Am. 2013;95(8):694–701. doi:10.2106/JBJS.L.00285.
2. Axelrad TW, Kakar S, Einhorn TA. New technologies for the enhancement of skeletal repair. Injury. 2007;38(Suppl 1):S49–62. doi:10.1016/j.injury.2007.02.010.
3. Valimaki VV, Moritz N, Yrjans JJ, Dalstra M, Aro HT. Peripheral quantitative computed tomography in evaluation of bioactive glass incorporation with bone. Biomaterials. 2005;26(33):6693–703. doi:10.1016/j.biomaterials.2005.04.033.
4. Drosse I, Volkmer E, Capanna R, De Biase P, Mutschler W, Schieker M. Tissue engineering for bone defect healing: an update on a multi-component approach. Injury. 2008;39(Suppl 2):S9–20. doi:10.1016/S0020-1383(08)70011-1.
5. Giannoudis PV, Dinopoulos H, Tsiridis E. Bone substitutes: an update. Injury. 2005;36(Suppl 3):S20–7. doi:10.1016/j.injury.2005.07.029.
6. Dias AG, Lopes MA, Santos JD, Afonso A, Tsuru K, Osaka A, et al. In vivo performance of biodegradable calcium phosphate glass ceramics using the rabbit model: histological and SEM observation. J Biomater Appl. 2006;20(3):253–66. doi:10.1177/0885328206052466.
7. Dorozhkin S, Ajaal T. Toughening of porous bioceramic scaffolds by bioresorbable polymeric coatings. Proc Inst Mech Eng H. 2009;223(4):459–70.
8. Hutmacher DW, Schantz JT, Lam CX, Tan KC, Lim TC. State of the art and future directions of scaffold-based bone engineering from a biomaterials perspective. J Tissue Eng Regen Med. 2007;1(4):245–60. doi:10.1002/term.24.
9. Hench LL, Xynos ID, Edgar AJ, Buterry LDK, Polak JM, Zhong J-P, et al. Gene activating glasses. J Inorg Mater. 2002;17(5):897–909.
10. Hench LL, Polak JM. Third-generation biomedical materials. Science. 2002;295(5557):1014–7. doi:10.1126/science.1067404.
11. Xynos ID, Edgar AJ, Buttery LD, Hench LL, Polak JM. Ionic products of bioactive glass dissolution increase proliferation of human osteoblasts and induce insulin-like growth factor II mRNA expression and protein synthesis. Biochem Biophys Res Commun. 2000;276(2):461–5. doi:10.1006/bbrc.2000.3503.
12. Hench LL. The story of bioglass. J Mater Sci Mater Med. 2006;17(11):967–78. doi:10.1007/s10856-006-0432-z.
13. Mastrogiacomo M, Scaglione S, Martinetti R, Dolcini L, Beltrame F, Cancedda R, et al. Role of scaffold internal structure on in vivo bone formation in macroporous calcium phosphate bioceramics. Biomaterials. 2006;27(17):3230–7. doi:10.1016/j.biomaterials.2006.01.031.
14. Spector M. Biomaterials-based tissue engineering and regenerative medicine solutions to musculoskeletal problems. Swiss Med Wkly. 2006;136(19–20):293–301. doi:10.2006/19/smw-11310.
15. Wu C, Zhu Y, Chang J, Zhang Y, Xiao Y. Bioactive inorganic-materials/alginate composite microspheres with controllable drug-delivery ability. J Biomed Mater Res B Appl Biomater. 2010;94(1):32–43. doi:10.1002/jbm.b.31621.
16. Boccaccini AR, Maquet V. Bioresorbable and bioactive polymer/Bioglass® composites with tailored pore structure for tissue engineering applications. Compos Sci Technol. 2003;63(16):2417–29. doi:10.1016/S0266-3538(03)00275-6.
17. Pascu EI, Stokes J, McGuinness GB. Electrospun composites of PHBV, silk fibroin and nano-hydroxyapatite for bone tissue engineering. Mater Sci Eng C Mater Biol Appl. 2013;33(8):4905–16. doi:10.1016/j.msec.2013.08.012.
18. Poologasundarampillai G, Wang D, Li S, Nakamura J, Bradley R, Lee PD, et al. Cotton-wool-like bioactive glasses for bone regeneration. Acta Biomater. 2014;10(8):3733–46. doi:10.1016/j.actbio.2014.05.020.
19. Lin Y, Brown RF, Jung SB, Day DE. Angiogenic effects of borate glass microfibers in a rodent model. J Biomed Mater Res A. 2014;102(12):4491–9. doi:10.1002/jbm.a.35120.
20. Souza MT, Zanotto ED, Peitl-Filho O. Vitreous composition, bioactive glassy fibers and tissues. Patent Application No. BR 10 2013 020961 9. Universidade Federal de São Carlos, Brazil, 2013.
21. Oliveira P, Ribeiro DA, Pipi EF, Driusso P, Parizotto NA, Renno AC. Low level laser therapy does not modulate the outcomes of a highly bioactive glass-ceramic (Biosilicate) on bone consolidation in rats. J Mater Sci Mater Med. 2010;21(4):1379–84. doi:10.1007/s10856-009-3945-4.
22. Bossini PS, Renno AC, Ribeiro DA, Fangel R, Peitl O, Zanotto ED, et al. Biosilicate(R) and low-level laser therapy improve bone repair in osteoporotic rats. J Tissue Eng Regen Med. 2011;5(3):229–37. doi:10.1002/term.309.
23. Pedrosa WF Jr, Okamoto R, Faria PE, Arnez MF, Xavier SP, Salata LA. Immunohistochemical, tomographic and histological study on onlay bone graft remodeling. Part II: calvarial bone. Clin Oral Implants Res. 2009;20(11):1254–64. doi:10.1111/j.1600-0501.2009.01747.x.
24. Matsumoto MA, Caviquioli G, Biguetti CC, Holgado LA, Saraiva PP, Renno ACM, Kawakami RY. A novel bioactive vitroceramic presents similar biological responses as autogenous bone grafts. J Mater Sci Mater Med. 2012;23(6):1447–56. doi:10.1007/s10856-012-4612-8.
25. Abiraman S, Varma HK, Kumari TV, Umashankar PR, John A. Preliminary in vitro and in vivo characterizations of a sol–gel derived bioactive glass–ceramic system. Bull Mater Sci. 2002;25(5):419–29.
26. Schepers EJ, Ducheyne P. Bioactive glass particles of narrow size range for the treatment of oral bone defects: a 1-24 month experiment with several materials and particle sizes and size ranges. J Oral Rehabil. 1997;24(3):171–81.
27. Ruhe PQ, Boerman OC, Russel FG, Mikos AG, Spauwen PH, Jansen JA. In vivo release of rhBMP-2 loaded porous calcium phosphate cement pretreated with albumin. J Mater Sci Mater Med. 2006;17(10):919–27. doi:10.1007/s10856-006-0181-z.
28. Qi X, Ye J, Wang Y. Improved injectability and in vitro degradation of a calcium phosphate cement containing poly(lactide-co-glycolide) microspheres. Acta Biomater. 2008;4(6):1837–45. doi:10.1016/j.actbio.2008.05.009.
29. Gu Y, Chen L, Yang HL, Luo ZP, Tang TS. Evaluation of an injectable silk fibroin enhanced calcium phosphate cement loaded with human recombinant bone morphogenetic protein-2 in ovine lumbar interbody fusion. J Biomed Mater Res A. 2011;97(2):177–85. doi:10.1002/jbm.a.33018.

30. van de Watering FC, van den Beucken JJ, Walboomers XF, Jansen JA. Calcium phosphate/poly(D, L-lactic-co-glycolic acid) composite bone substitute materials: evaluation of temporal degradation and bone ingrowth in a rat critical-sized cranial defect. Clin Oral Implants Res. 2012;23(2):151–9. doi:10.1111/j.1600-0501.2011.02218.x.
31. Hench LL, Xynos ID, Polak JM. Bioactive glasses for in situ tissue regeneration. J Biomater Sci Polym Ed. 2004;15(4):543–62.
32. Valimaki VV, Aro HT. Molecular basis for action of bioactive glasses as bone graft substitute. Scand J Surg. 2006;95(2):95–102.
33. Moura J, Teixeira LN, Ravagnani C, Peitl O, Zanotto ED, Beloti MM, et al. In vitro osteogenesis on a highly bioactive glass-ceramic (Biosilicate). J Biomed Mater Res A. 2007;82(3):545–57. doi:10.1002/jbm.a.31165.
34. Renno AC, van de Watering FC, Nejadnik MR, Crovace MC, Zanotto ED, Wolke JG, et al. Incorporation of bioactive glass in calcium phosphate cement: an evaluation. Acta Biomater. 2013;9(3):5728–39. doi:10.1016/j.actbio.2012.11.009.
35. Zhang XS, Zhang X, Schwarz EM, Young DA, Puzas JE, Rosier RN, O'keefe RJ. Cyclooxygenase-2 regulates mesenchymal cell differentiation into the osteoblast lineage and is critically involved in bone repair. J Clin Invest. 2002;109(11):1405–15. doi:10.1172/JCI15681.
36. Afzal F, Polak J, Buttery L. Endothelial nitric oxide synthase in the control of osteoblastic mineralizing activity and bone integrity. J Pathol. 2004;202(4):503–10. doi:10.1002/path.1536.
37. Lemaire V, Tobin FL, Greller LD, Cho CR, Suva LJ. Modeling the interactions between osteoblast and osteoclast activities in bone remodeling. J Theor Biol. 2004;229(3):293–309. doi:10.1016/j.jtbi.2004.03.023.
38. Kearns AE, Khosla S, Kostenuik PJ. Receptor activator of nuclear factor kappaB ligand and osteoprotegerin regulation of bone remodeling in health and disease. Endocr Rev. 2008;29(2):155–92. doi:10.1210/er.2007-0014.
39. Anandarajah AP. Role of RANKL in bone diseases. Trends Endocrinol Metab. 2009;20(2):88–94. doi:10.1016/j.tem.2008.10.007.
40. Pinto KN, Tim CR, Crovace MC, Matsumoto MA, Parizotto NA, Zanotto ED, et al. Effects of biosilicate((R)) scaffolds and low-level laser therapy on the process of bone healing. Photomed Laser Surg. 2013;31(6):252–60. doi:10.1089/pho.2012.3435.
41. Kondo N, Ogose A, Tokunaga K, Ito T, Arai K, Kudo N, et al. Bone formation and resorption of highly purified beta-tricalcium phosphate in the rat femoral condyle. Biomaterials. 2005;26(28):5600–8. doi:10.1016/j.biomaterials.2005.02.026.
42. Saino E, Grandi S, Quartarone E, Maliardi V, Galli D, Bloise N, et al. In vitro calcified matrix deposition by human osteoblasts onto a zinc-containing bioactive glass. Eur Cell Mater. 2011;21:59–72 discussion.
43. Valerio P, Pereira MM, Goes AM, Leite MF. The effect of ionic products from bioactive glass dissolution on osteoblast proliferation and collagen production. Biomaterials. 2004;25(15):2941–8. doi:10.1016/j.biomaterials.2003.09.086.
44. Granito RN, Ribeiro DA, Renno AC, Ravagnani C, Bossini PS, Peitl-Filho O, et al. Effects of biosilicate and bioglass 45S5 on tibial bone consolidation on rats: a biomechanical and a histological study. J Mater Sci Mater Med. 2009;20(12):2521–6. doi:10.1007/s10856-009-3824-z.
45. Bosch C, Melsen B, Vargervik K. Importance of the critical-size bone defect in testing bone-regenerating materials. J Craniofac Surg. 1998;9(4):310–6.